

See discussions, stats, and author profiles for this publication at: <https://www.researchgate.net/publication/363328726>

Solving the Electric Capacitated Vehicle Routing Problem with Cargo Weight

Conference Paper · July 2022

DOI: 10.1109/CEC55065.2022.9870383

CITATIONS

0

READS

148

4 authors, including:



[Michalis Mavrovouniotis](#)

Cyprus University of Technology

70 PUBLICATIONS 2,453 CITATIONS

[SEE PROFILE](#)



[Changhe Li](#)

China University of Geosciences

112 PUBLICATIONS 4,257 CITATIONS

[SEE PROFILE](#)



[Georgios Ellinas](#)

University of Cyprus

361 PUBLICATIONS 4,462 CITATIONS

[SEE PROFILE](#)

Solving the Electric Capacitated Vehicle Routing Problem with Cargo Weight

Michalis Mavrovouniotis

*KIOS Research and Innovation Center of Excellence
Department of Electrical and Computer Engineering
University of Cyprus
Nicosia, Cyprus.
mavrovouniotis.michalis@ucy.ac.cy*

Changhe Li

*School of Automation
China University of Geosciences
Hubei Key Laboratory of Advanced Control and
Intelligent Automation for Complex Systems
Wuhan, China.
changhe.li@gmail.com*

Georgios Ellinas

*KIOS Research and Innovation Center of Excellence
Department of Electrical and Computer Engineering
University of Cyprus
Nicosia, Cyprus.
gellinas@ucy.ac.cy*

Marios Polycarpou

*KIOS Research and Innovation Center of Excellence
Department of Electrical and Computer Engineering
University of Cyprus
Nicosia, Cyprus.
mpolycar@ucy.ac.cy*

Abstract—Electric vehicle routing problems are challenging variations of the traditional vehicle routing problem which incorporate the possibility of electric vehicle (EV) recharging at any station, while satisfying the delivery demands of customers. This work addresses the recently formulated capacitated vehicle routing problem (E-CVRP) with variable energy consumption rate. In particular, the cargo weight, which is one of the main factors affecting the energy consumption rate of EVs, is considered (i.e., the heavier the EV the higher the rate). As a solution method, an ant colony optimization algorithm with a local search heuristic is developed. Experiments are conducted on a recently generated benchmark set of E-CVRP instances demonstrating that the performance of the proposed technique improves on the best known so far solutions.

Index Terms—Electric vehicle, capacitated vehicle routing problem, ant colony optimization

I. INTRODUCTION

Vehicle routing problems (VRPs) are difficult \mathcal{NP} -hard combinatorial optimization problems [1]. The VRP variations in which EVs are utilized incorporate additional hard constraints that impose more challenges to the optimizer. Similar with most \mathcal{NP} -hard combinatorial optimization problems, electric vehicle routing problems (EVRPs) are straightforward to describe but difficult to solve [2]. The main objective in EVRPs is to find the best possible routes for a fleet of electric vehicles so that the delivery demands of a set of customers are satisfied, while ensuring that the EVs will never run out of energy.

In the last few years, several EVRP variations have emerged that mainly differ on their constraints such as the EVRP with

time windows [3], [4], the EVRP with pick up and delivery [5], the EVRP with multiple depots [6], the EVRP with service times [7], and the EVRP with backhauls [8]. Refer to the comprehensive survey in [9] for further details.

The common characteristic of all EVRP variations, is that EVs are able to perform visit(s) to recharging station(s) due to their limited driving range. In [10] (2020 Congress on Evolutionary Computation competition for the Electric Vehicle Routing Problem – <https://mavrovouniotis.github.io/EVRPcompetition2020/>), the electric capacitated vehicle routing problem (E-CVRP) with fixed energy consumption rate was formulated. Later on, the E-CVRP with variable energy consumption was introduced [11]. Considering that each EV has a limited cargo load to satisfy the delivery demands of the customers, the energy consumption rate of the EV is proportional to that cargo load. In other words, the heavier the EV the higher the energy consumption rate, and hence, more energy will be consumed. There are other minor factors that may affect the energy consumption rate (such as environmental factors [7]), but the focus in this work is on the weight of the EV (including the cargo), as this is one of the most important factors affecting energy consumption [12].

In this work, the E-CVRP model with variable energy consumption proposed in [11] is adopted, as it fits better to real-world applications. Since the E-CVRP is a variation of the well-known capacitated vehicle routing problem, the high complexity of the problem makes exact solution methods impractical [1]. To address the E-CVRP, an ant colony optimization (ACO) metaheuristic [13] together with a local search heuristic are designed. The combination of these two techniques has been successfully used to solve world-scale instances of similar vehicle routing problems [14], [15].

This work was supported by the European Union's Horizon 2020 Research and Innovation Programme under Grant 739551 (KIOS CoE - TEAMING) and by the Republic of Cyprus through the Deputy Ministry of Research, Innovation and Digital Policy.

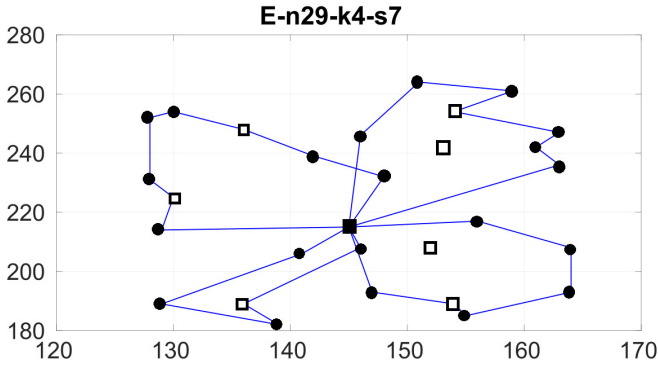


Fig. 1: Illustration of the optimal solution of the E-n29-k4-s7 problem instance. The black square represents the central depot, the black circles the customers and the white squares the charging stations.

Experiments are conducted on a set of recently generated E-CVRP benchmark instances, with the results showing that the proposed method improves several previous best-known solutions.

The rest of the paper is organized as follows. Section II describes the E-CVRP with cargo weight, while Section III describes the ACO with local search heuristic designed to solve the E-CVRP. Experimental results obtained on a recently generated benchmark set of E-CVRP instances are presented in Section IV. Section V presents concluding remarks and possible future research avenues.

II. THE ELECTRIC CAPACITATED VEHICLE ROUTING PROBLEM

As previously mentioned, the E-CVRP with variable energy consumption rate (proportional to the cargo weight of the EV) was recently formulated in [11]. The particular model differs from the previous E-CVRP model proposed in [10] in which fixed energy consumption rate was considered.

The E-CVRP with cargo weight is modeled using a complete weighted graph $G = (N, A)$, where $N = \{0\} \cup I \cup F'$ is a set of nodes and $A = \{(i, j) \mid i, j \in N, i \neq j\}$ is a set of arcs connecting these nodes. A non-negative value d_{ij} is associated with each arc which represents the Euclidean distance between nodes i and j . Node 0 denotes the central depot. The set $I \subset N$ denotes the set of customers, where each customer $i \in I$ is assigned a positive value δ_i indicating the customer's delivery demand. The set $F' \subset N$ denotes the set of β_i node copies of each charging station $i \in F$ (i.e., $|F'| = \sum_{i \in F} \beta_i$) to allow multiple visits (if required) for EVs to each charging station $i \in F'$ [16]. The upper bound on the number of node copies for each charging station is equal to $\beta_i = 2|I|$, because in the worst case one EV for each customer is needed and a visit to a charging station before and after serving each customer is required [17].

Each EV consists of: (i) a cargo load capacity, u_i ($0 \leq u_i \leq C$), and (ii) a battery charge level y_i ($0 \leq y_i \leq Q$), where C and Q are the maximal cargo and the maximal battery

charge level of the EV respectively, and u_i and y_i are the cargo load and battery charge level of an EV on arrival at node i , respectively. For each traveled arc (i, j) an EV consumes $h_i d_{ij}$ of the remaining battery charge level, where h_i is the variable energy consumption rate [11] of an EV defined as:

$$h_i = r + u_i/C, \quad (1)$$

where r is a constant value representing the energy consumption rate of an EV with no cargo. The variable energy consumption rate is proportional to the current cargo weight of the EV, i.e., the heavier the cargo weight the higher the consumption rate. The reader should note that h_i is different at each node i as the cargo load changes due to deliveries.

Fig. 1 shows an example of a solution consisting of the best possible routes for four EVs for the E-n29-k4-s7 problem instance [11]. Three routes consist of one charging station visit and one route consists of two charging station visits. Note that the term "routes" is used instead of the term "EVs", since the solution can be operated either by four EVs simultaneously or by a single EV sequentially.

The mathematical model of E-CVRP is defined as follows:

$$\min \sum_{i \in N, j \in N, i \neq j} d_{ij} x_{ij}, \quad (2)$$

s.t.

$$\sum_{j \in N, i \neq j} x_{ij} = 1, \forall i \in I, \quad (3)$$

$$\sum_{j \in N, i \neq j} x_{ij} \leq 1, \forall i \in F', \quad (4)$$

$$\sum_{j \in N, i \neq j} x_{ij} - \sum_{j \in N, i \neq j} x_{ji} = 0, \forall i \in N, \quad (5)$$

$$u_j \leq u_i - \delta_j x_{ij} + C(1 - x_{ij}), \forall i \in N, \forall j \in N, i \neq j, \quad (6)$$

$$u_j \geq u_i - \delta_j x_{ij} - C(1 - x_{ij}), \forall i \in N, \forall j \in N, i \neq j, \quad (7)$$

$$0 \leq u_i \leq C, \forall i \in N, \quad (8)$$

$$u_0 = C, \quad (9)$$

$$y_j \leq y_i - h_i d_{ij} x_{ij} + Q(1 - x_{ij}), \forall i \in I, \forall j \in N, i \neq j, \quad (10)$$

$$y_j \leq Q - h_i d_{ij} x_{ij}, \forall i \in F', \forall j \in N, i \neq j, \quad (11)$$

$$0 \leq y_i \leq Q, \forall i \in N, \quad (12)$$

$$y_0 = Q, \quad (13)$$

$$x_{ij} \in \{0, 1\}, \forall i \in N, \forall j \in N, i \neq j, \quad (14)$$

where Eq. (2) defines the E-CVRP objective function to minimize the total distance of the routes, Eq. (3) ensures that each customer is visited exactly once, Eq. (4) handles the multiple visits of EVs to recharging stations, Eq. (5) establishes the flow conservation by guaranteeing that at each node the number of incoming arcs is equal to the number of outgoing arcs, Eq. (6), Eq. (7) and Eq. (8) guarantee delivery demand fulfillment at all customers by assuring a non-negative cargo load capacity upon arrival at any node, Eq. (9) ensures

that EVs start with full cargo load from the depot, Eq. (10), Eq. (11) and Eq. (12) ensure that the battery charge level never falls below 0, Eq. (13) ensures that EVs start fully charged from the depot, and Eq. (14) is the binary decision variable denoting whether arc (i, j) is traversed (i.e., $x_{ij} = 1$) or not (i.e., $x_{ij} = 0$).

III. ANT COLONY OPTIMIZATION WITH LOCAL SEARCH FOR THE E-CVRP

The combination of metaheuristics (e.g., ACO) with local search heuristics is one of the best techniques in solving difficult optimization problems efficiently [18]–[21]. Algorithm 1 gives the main procedures (described in detail in the following subsections) of the proposed combination.

A. $\mathcal{MAX-MIN}$ Ant System (\mathcal{MMAS})

In this work, the $\mathcal{MAX-MIN}$ Ant System (\mathcal{MMAS}) [22] variant is utilized which is one of the most-studied ACO variants and has already proven its good performance on relevant EVRPs [7], [23]–[25].

1) *Initialization*: All the arcs (i, j) of the problem are associated with a pheromone trail value τ_{ij} and a heuristic information value η_{ij} . The former value is uniformly initialized as follows: $\tau_{ij} \leftarrow \tau_0, \forall (i, j) \in A$, where τ_0 is the initial pheromone trail value. The latter value is the inverse of the arc weight defined as follows: $\eta_{ij} = 1/d_{ij}, \forall (i, j) \in A$.

2) *Solution Construction*: A colony of ω ants always start at the central depot, i.e., node 0. Then, each ant k makes selections (node by node) biased by the existing pheromone trail and heuristic information values associated with the arc (i, j) until all nodes from customer set I are selected.

The probability distribution with which ant k selects node j from node i is defined as follows:

$$p_{ij}^k = \begin{cases} \frac{[\tau_{ij}]^\alpha [\eta_{ij}]^\beta}{\sum_{l \in \mathcal{N}_i^k} [\tau_{il}]^\alpha [\eta_{il}]^\beta}, & \text{if } j \in \mathcal{N}_i^k, \\ 0, & \text{otherwise,} \end{cases} \quad (15)$$

where τ_{ij} and η_{ij} are, respectively, the existing pheromone trail and the heuristic information available a priori associated with arc (i, j) . Parameters α and β determine the relative influence of τ_{ij} and η_{ij} , respectively, while \mathcal{N}_i^k is the set of unselected nodes (from customer set I) for the k -th ant adjacent to node i . Note that the depot and charging station nodes are not included in the \mathcal{N}_i^k set but they are selected independently (described in the following) to satisfy the constraints of the E-CVRP.

The procedure proposed in [11] is used to construct a feasible E-CVRP solution T^k (i.e., the routes of all EVs) as follows. Each customer $j \in \mathcal{N}_i^k$ available for selection at any construction step must satisfy the following criteria: (a) the delivery demand of customer j must not violate the capacity constraint, (b) the required energy to travel to customer j from node (either charging station, depot or customer) i must not violate the energy constraint, and (c) customer j must have at least one charging station or the depot within its energy range [7]. The procedure to build a feasible E-CVRP solution is presented in Algorithm 2.

Algorithm 1 \mathcal{MMAS} with Local Search

```

1: Initialization
2: while termination condition is satisfied do
3:   Construct Solutions
4:   Local Search
5:   Update Best
6:   Update Statistics
7:   Update Pheromone Trails
8: end while

```

Algorithm 2 E-CVRP Solution Construction

```

1:  $T^k \leftarrow$  insert depot  $\{0\}$  at position 0
2:  $step \leftarrow 1$ 
3: while ant  $k$  has not selected all customers do
4:    $i \leftarrow$  find current node from  $T^k$  at position  $step - 1$ 
5:    $j \leftarrow$  select probabilistically next customer from  $\mathcal{N}_i^k$ 
6:    $step \leftarrow step + 1$ 
7:   if customer  $j$  violates capacity constraint then
8:      $T^k \leftarrow$  insert depot  $\{0\}$  at position  $step$ 
9:   else if customer  $j$  violates energy constraints then
10:     $s \leftarrow$  select closest station between customers  $i$  and  $j$ 
11:     $T^k \leftarrow$  insert  $s$  at position  $step$ 
12:   else
13:     $T^k \leftarrow$  insert  $j$  at position  $step$ 
14:   end if
15: end while
16:  $T^k \leftarrow$  insert depot  $\{0\}$  at position  $step + 1$ 

```

In case the selected customer j violates the cargo load capacity, then the depot node is inserted (assuming that enough energy is available to travel back to the depot) to the T^k solution to close the route of the EV. Moreover, in case the selected customer j violates either the energy constraint or the energy range criteria, then the closest energy recharging station s between node i and potential next customer j is selected as follows:

$$s = \arg \min_{l \in F} \{d_{il} + d_{lj}\}, \quad (16)$$

and inserted to the T^k solution. A charging station s is also selected using Eq. (16) when not enough energy is available to travel back to the depot. Note that the possibility of not having enough energy to travel to any energy recharging station or back to the central depot is eliminated because of the energy range criteria imposed in the selection of customers.

3) *Pheromone Update*: In the \mathcal{MMAS} variant [22], [26], [27], the pheromone trails are updated by first decreasing the pheromone trails on all arcs (using pheromone evaporation), and then increasing the pheromone trails on the arcs of the solution constructed by the best ant (using pheromone deposit). The pheromone evaporation is applied as follows:

$$\tau_{ij} \leftarrow (1 - \rho)\tau_{ij}, \forall (i, j) \in A, \quad (17)$$

where ρ ($\rho \in (0, 1]$) is the evaporation rate.

After pheromone evaporation, the best ant deposits pheromone on the arcs of its solution components as follows:

$$\tau_{ij} \leftarrow \tau_{ij} + \Delta\tau_{ij}^{best}, \forall (i, j) \in T^{best}, \quad (18)$$

where $\Delta\tau_{ij}^{best} = 1/C^{best}$ is the amount of pheromone that the best ant deposits and C^{best} is the quality of the best solution T^{best} . The “best” ant that is allowed to deposit pheromone may be either the best-so-far ant (i.e., the ant representing the best solution from all iterations so far), in which $C^{best} = C^{bs}$, or the iteration-best ant, in which case $C^{best} = C^{ib}$. These two ants are updated in line 5 of Algorithm 1 and they are allowed to deposit pheromone accordingly in an alternate way [27]. More precisely, the best-so-far ant is allowed to deposit pheromone every f^{bs} iterations whereas in the rest of the iterations it is the iteration-best ant that deposits pheromone.

Furthermore, lower and upper limits of the pheromone trail values are explicitly imposed as follows:

$$\tau_{ij} \leftarrow \begin{cases} \tau_{max}, & \text{if } \tau_{ij} > \tau_{max}, \\ \tau_{min}, & \text{if } \tau_{ij} < \tau_{min}, \\ \tau_{ij}, & \text{otherwise,} \end{cases} \quad \forall (i, j) \in A, \quad (19)$$

where τ_{min} and τ_{max} are, respectively, the minimum and maximum pheromone trails. In addition, all the pheromone trails are uniformly re-initialized to the τ_{max} value whenever the stagnation behavior (i.e., when all ants construct the same solution for several iterations) occurs or when no improved solution is found for a given number of iterations (line 6 in Algorithm 1). The stagnation behavior is detected using the λ -branching factor that measures the distribution of the pheromone trail values [28].

B. Local Search

For all ACO constructed solutions the following local search operators are applied: *exchange*, *relocate*, *2-opt* and *2-opt**. The exchange operator swaps the location of two nodes whereas the relocate operator moves one node to a different location [29]. Suppose that the exchange operator is applied to nodes i and j as shown in Fig. 2(a). This will cause arcs $(j-1, j)$, $(j, j+1)$, $(i-1, i)$, and $(i, i+1)$ to be removed, and arcs $(i, j+1)$, $(j-1, i)$, $(j, i+1)$, and $(i-1, j)$ to be inserted. Also, suppose that the relocate operator is applied to node i for the position next to node j as shown in Fig. 2(b). This will cause arcs $(j, j+1)$, $(i-1, i)$, and $(i, i+1)$ to be removed, and arcs $(i-1, i+1)$, (j, i) , and $(i, j+1)$ to be inserted. Both operators are used as intra-route (involves a single route as presented in Fig. 2) and inter-route (involves two routes as presented in Fig. 3) moves. Exactly the same arcs will be affected for the corresponding inter-route moves as described previously. The 2-opt operator [30] shown in Fig. 4(a) removes arcs $(j, j+1)$ and $(i-1, i)$ and inserts arcs $(i, j+1)$ and $(j, i-1)$. The 2-opt* operator [31] shown in Fig. 4(b) removes arc $(i, i+1)$ from one route and arc $(j, j+1)$ from another route and inserts arc $(j, i+1)$ in the former route and arc $(i, j+1)$ in the latter route. The 2-opt operator is only used

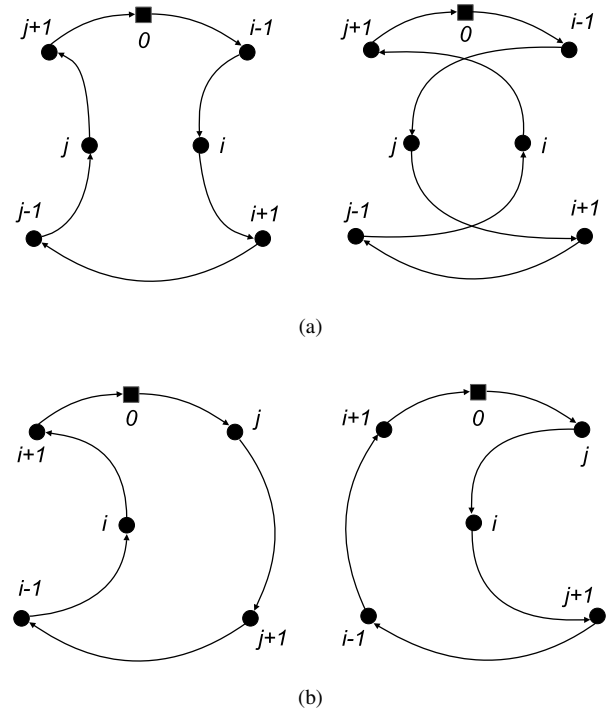


Fig. 2: (a) Exchange and (b) relocate intra-route moves within the same route. The black square represents the central depot and the black circles the customers.

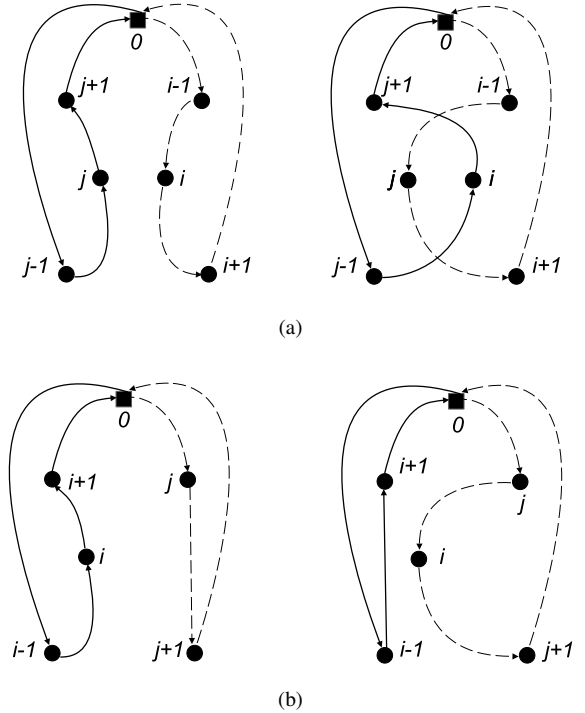


Fig. 3: (a) Exchange and (b) relocate inter-route moves from two different routes. The black square represents the central depot and the black circles the customers.

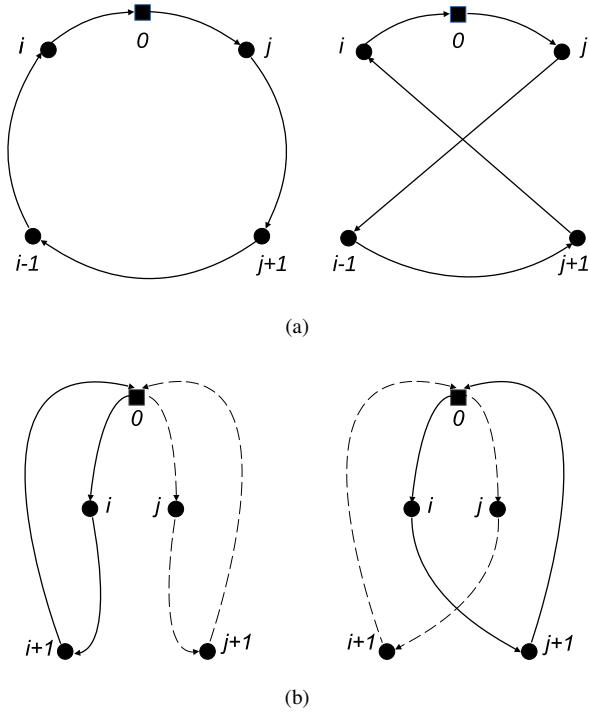


Fig. 4: (a) 2-opt intra-route move within the same route and (b) 2-opt* inter-route move from two different routes. The black square represents the central depot and the black circles the customers.

for intra-route moves whereas the 2-opt* operator is only used for inter-route moves.

Note that, only moves that do not violate the capacity constraint are allowed for the inter-route moves, while intra-route moves do not violate the capacity constraint. On the contrary, both type of moves may violate the energy constraint, since the charging stations may change positions, or the current position of the stations is affected due to the changes caused in the order of the customers. Therefore, recharging stations are not selected for exchange and relocate moves, but they are allowed in 2-opt and 2-opt* moves. In this way, the probability of violating the energy constraint will be minimized. However, in case a solution violates the energy constraint, the affected routes of the E-CVRP solution are repaired by inserting new station(s) or removing existing station(s) to satisfy the energy constraint using Eq. 16.

All local search operators are applied until no further improvement is possible, as presented in Algorithm 3, in a cyclic way [32]. It must be noted that the pheromone trails are updated after the local search improvements to mark them in the pheromone trails so they can be exploited in the next iterations (lines 3 – 4 in Algorithm 1).

IV. EXPERIMENTAL RESULTS

A. Experimental Setup

The MMAS with local search (MMAS+ls) performs 25000n evaluations of complexity $\mathcal{O}(n^2)$ as proposed for

Algorithm 3 Local Search

```

1:  $C^k \leftarrow$  calculate solution quality of  $T^k$ 
2: while solution quality is improved do
3:    $T^{k'} \leftarrow$  apply exchange, relocate, 2-opt, and 2-opt* to  $T^k$ 
4:   if energy constraint violated then
5:      $T^{k'} \leftarrow$  insert or remove charging station(s)
6:   end if
7:    $C^{k'} \leftarrow$  calculate solution quality of  $T^{k'}$ 
8:   if  $C^{k'}$  is better than  $C^k$  then
9:      $T^k \leftarrow T^{k'}$ 
10:     $C^k \leftarrow C^{k'}$ 
11:   end if
12: end while

```

the 2020 Congress on Evolutionary Computation competition for the Electric Vehicle Routing Problem [10]. The partial evaluations required when applying the local search are added to the total evaluations of the algorithm. Ten independent runs are executed with different random seeds. For each run the total distance traveled for the solution with the best quality is recorded.

1) *E-CVRP Benchmark Instances*: The recently generated E-CVRP benchmark instances (available at https://github.com/KIOS-Research/e-cvrp_benchmark_instances) are used in the experiments. This set of benchmark instances is generated by utilizing existing CVRP instances using the conversion method (with γ and ϕ parameters set to $\gamma = 2$ and $\phi = 0.125$, respectively) described in [11]. For more details refer to the relevant reference. Note that the benchmark instances used in this work (with variable energy consumption rate) are different from the benchmark instances (with fixed energy consumption rate) proposed in [10].

2) *Parameter Tuning*: MMAS with local search is configured following the guidelines of [22]. The colony size is set to $\omega = 25$ ants for problem instances with size $n < 400$ and $\omega = 50$ ants for problem instances with size $n > 400$. The evaporation rate is set to $\rho = 0.2$, the initial pheromone trail value is set to $\tau_0 = 1/\rho C^{nn}$, the upper and lower pheromone trails limits are set to $\tau_{max} = 1/\rho C^{bs}$ and $\tau_{min} = \tau_{max}/(2n)$, respectively. Note that C^{nn} is the solution quality of the solution generated by the nearest-neighbor heuristic. The two parameters of the decision rule are set to $\alpha = 1$ and $\beta = 2$. The frequency with which the best-so-far ant is allowed to deposit pheromone is set as follows:

$$f^{bs} = \begin{cases} \infty, & \text{if } t \leq 25, \\ 5, & \text{if } 26 \leq t \leq 75, \\ 3, & \text{if } 76 \leq t \leq 125, \\ 2, & \text{if } 126 \leq t \leq 250, \\ 1, & \text{otherwise,} \end{cases} \quad (20)$$

where t is the iteration counter of the algorithm. The schedule is tuned as proposed in [27], that is, to gradually shift the

TABLE I: Best solution quality found in 10 runs obtained from the \mathcal{MMAS} with local search on the E-CVRP benchmark set. The best known solutions (BKS) are taken from [11].

E-CVRP instance	BKS	$\mathcal{MMAS}+ls$		
		#charges	#routes	best
E-n29-k4-s7	383[†]	4	4	383
E-n30-k3-s7	577[†]	5	3	577
E-n35-k3-s5	527[†]	4	3	527
E-n37-k4-s4	865	4	4	857
E-n60-k5-s9	544	7	5	537
E-n89-k7-s13	724	8	7	711
E-n112-k8-s11	860	7	8	845
M-n110-k10-s9	914	6	10	876
M-n126-k7-s5	1099	4	7	1094
M-n163-k12-s12	1109	10	12	1088
M-n212-k16-s12	1398	12	17	1386
F-n49-k4-s4	740	1	4	746
F-n80-k4-s8	240	5	4	239
F-n140-k7-s5	1229	2	7	1210
X-n147-k7-s4	17704	5	7	17345
X-n221-k11-s9	12235	8	12	12130
X-n360-k40-s9	27701	9	41	27327
X-n469-k26-s10	26881	16	27	26763
X-n577-k30-s4	55266	32	30	54779
X-n698-k75-s13	75048	45	78	74818
X-n759-k98-s10	84996	47	100	83204
X-n830-k171-s11	167575	97	179	166593
X-n920-k207-s4	345214	76	214	341599
X-n1006-k43-s5	80765	27	43	79635

[†] Optimal solution quality.
Best results are shown in **bold**.

emphasis from the iteration-best ant to the best-so-far ant for the pheromone update.

B. Comparison Against Best-Known Solutions

The experimental results of the \mathcal{MMAS} with local search are given in Table I for 24 E-CVRP benchmark instances. For each instance the numbers after n, k, and s letters in the instance name identifies the size of the problem, the minimum number of routes, and the number of charging stations, respectively. Since the benchmark set is recent, there are no other existing methods to compare, except the initial best known solutions (BKS) reported in [11]. The term “best” denotes the best solution found by \mathcal{MMAS} with local search from its 10 independent executions. Further, “#charges” and “#routes” denote the number of charges and routes that the best solution consists of.

From Table I it can be observed that the proposed \mathcal{MMAS} with local search is able to find the global optimum on solved instances E-n29-k4-s7, E-n30-k3-s7, and E-n35-k3-s5 in which the optimum is known. On the remaining (unsolved) instances the proposed \mathcal{MMAS} is able to find better solutions than most of the BKS (except in F-n49-k-s4 instance). The percentage deviation of the proposed method from the BKS solution is in the worst case 0.83%. On the other hand, the proposed method improves the BKS with a percentage deviation up to -4.15%.

TABLE II: Mean solution quality and standard deviation averaged over 10 runs obtained from the \mathcal{MMAS} with and without local search on the E-CVRP benchmark set.

E-CVRP instance	\mathcal{MMAS}	$\mathcal{MMAS}+ls$
E-n29-k4-s7	384.5±0.7	383.0±0.0
E-n30-k3-s7	582.0±0.0	577.0±0.0
E-n35-k3-s5	533.0±1.4	528.9±2.1
E-n37-k4-s4	868.5±1.6	857.8±0.4
E-n60-k5-s9	557.0±6.4	539.9±4.0
E-n89-k7-s13	739±2.9	722.6±8.3
E-n112-k8-s11	878.3±14.6	853.9±9.6
M-n110-k10-s9	923.7±9.7	886.2±6.8
M-n126-k7-s5	1103.6±5.7	1094.3±0.6
M-n163-k12-s12	1129.2±8.9	1106.7±13.0
M-n212-k16-s12	1419.2±11.8	1412.8±15.8
F-n49-k4-s4	775.7±6.9	748.0±1.1
F-n80-k4-s8	243.9±2.8	239.5±1.5
F-n140-k7-s5	1233.8±2.9	1215.3±4.1
X-n147-k7-s4	17792.3±89.7	17604.0±176.4
X-n221-k11-s9	12487.9±109.4	12339.5±194.6
X-n360-k40-s9	28034.4±168.6	27601.6±180.9
X-n469-k26-s10	27391.7±257.0	27334.5±367.7
X-n577-k30-s4	55627.6±209.4	55329.0±368.3
X-n698-k75-s13	75646.6±323.7	75204.7±298.2
X-n759-k98-s10	85683.7±558.8	85429.8±382.5
X-n830-k171-s11	168465.0±376.1	167525.9±443.2
X-n920-k207-s4	346619.4±688.2	342856.5±303.3
X-n1006-k43-s5	81549.3±568.8	81217.8±432.4

C. Effect of the Local Search

The mean and standard deviation results (over 10 runs) of the \mathcal{MMAS} with and without local search are given in Table II for 24 E-CVRP benchmark instances. The comparisons in Table II demonstrate the effectiveness of combining \mathcal{MMAS} with the local search described in Section III-B, since in most problem instances the mean solution quality is better. To further support this claim, Fig. 5 gives the solution quality (averaged over 10 runs) as a function of algorithmic evaluations for \mathcal{MMAS} with and without the local search heuristic on four representative problem instances.

From Fig. 5 it can be observed that the \mathcal{MMAS} with local search maintains better solution quality than the \mathcal{MMAS} without local search from the early stages of the optimization process until the termination condition is reached. This is due to several reasons. ACO’s solution construction in Algorithm 2 utilizes a different neighborhood than the local search in Algorithm 3, and thus, the chance of a local search to improve the solutions constructed by ants is higher. In addition, a stand-alone local search typically starts from randomly generated solutions. Therefore, in complex and large search spaces it will be difficult to discover neighborhoods leading to high-quality solutions. The combination with ACO addresses this issue since the solutions will be provided by the ants. In fact, ACO is a global optimization method, that can guide local search heuristics to promising areas in the search space. In particular, ACO discovers neighborhoods that contain high-quality solutions for the local search to begin its search. The local search will explore the neighborhood until it reaches the

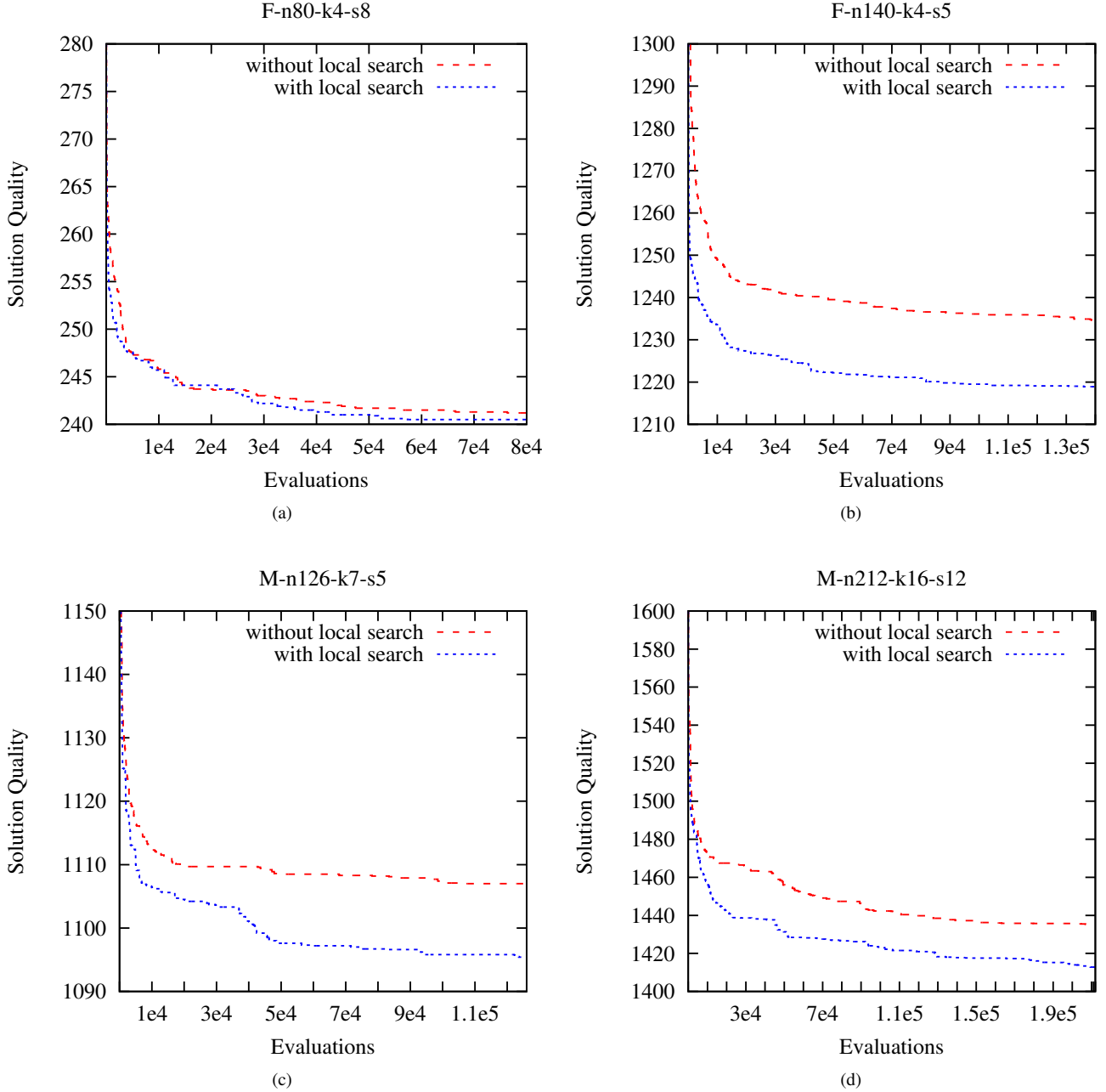


Fig. 5: Solution quality (averaged over 10 executions) as a function of algorithmic evaluations for \mathcal{MMAS} with and without the local search heuristic on the (a) F-n80-k4-s8, (b) F-n140-k4-s5, (c) M-n126-k7-s5, and (d) M-n212-k16-s12 problem instances.

local optimum (and possible the global optimum) solution.

D. Effect of Repairing Charging Stations

Table III gives the mean values of the \mathcal{MMAS} when the recharging station repair (see line 5 in Algorithm 3) is enabled in the proposed local search heuristic and when it is disabled. Recall, that the repair occurs when the resulting solutions from the local search improvements become infeasible due to violation of the energy constraint.

From Table III, it can be observed that when the repair of charging stations is enabled this leads to better results in most problem instances. This is the case because an infeasible solution may contain feasible routes that belong to the global optimum. Therefore, it would be beneficial to repair the infeasible route or routes, and thus, carry on with the local search improvement process.

TABLE III: Mean results of \mathcal{MMAS} with local search when the recharging station repair is enabled and when it is disabled.

E-CVRP instance	$\mathcal{MMAS}+ls$	
	enabled	disabled
E-n29-k4-s7	383.0 \pm 0.0	383.2 \pm 0.6
E-n30-k3-s7	577.0 \pm 0.0	578.0 \pm 0.0
E-n35-k3-s5	528.9 \pm 2.1	529.8 \pm 2.2
E-n37-k4-s4	857.8 \pm 0.4	857.9 \pm 0.3
E-n60-k5-s9	539.9 \pm 4.0	542.4 \pm 3.9
E-n89-k7-s13	722.6 \pm 8.3	733.4 \pm 8.2
E-n112-k8-s11	853.9 \pm 9.6	859.8 \pm 12.5

V. CONCLUSIONS

In this work, the E-CVRP with variable energy consumption rate is addressed. The energy consumption of the EVs is proportional to the current cargo load of the EVs, that is, the heavier the EV the more energy will be consumed. An ACO algorithm with a local search heuristic is designed to address the E-CVRP efficiently. The experimental results on a set of recently introduced benchmark set of E-CVRP instances demonstrate the good performance of the proposed method. In fact, new best known solutions are reported for several E-CVRP instances.

A future work direction involves the design of more advanced local search heuristics, since this technique has been proven effective in addressing E-CVRP.

REFERENCES

- [1] M. Garey and D. Johnson, *Computer and intractability: A guide to the theory of \mathcal{NP} -completeness*. San Francisco: Freeman, 1979.
- [2] F. Gonçalves, S. Cardoso, and S. Relvas, "Optimization of distribution network using electric vehicles: A VRP problem," University of Lisbon, Tech. Rep. CEG-IST, 2011.
- [3] M. Schneider, A. Stenger, and D. Goeke, "The electric vehicle-routing problem with time windows and recharging stations," *Transportation Science*, vol. 48, no. 4, pp. 500–520, 2014.
- [4] S. Rastani, T. Yüksel, and B. Çatay, *Electric Vehicle Routing Problem with Time Windows and Cargo Weight*. Cham: Springer International Publishing, 2020, pp. 175–190.
- [5] Q. Yang, D. Hu, H. Chu, and C. Xu, "An electric vehicle routing problem with pickup and delivery," in *CICTP 2018: Intelligence, Connectivity, and Mobility*, 2018, pp. 176–184.
- [6] J. Paz, M. Granada-Echeverri, and J. Escobar, "The multi-depot electric vehicle location routing problem with time windows," *International Journal of Industrial Engineering Computations*, vol. 9, pp. 123–136, 2018.
- [7] M. Mavrouniotis, G. Ellinas, and M. Polycarpou, "Ant colony optimization for the electric vehicle routing problem," in *2018 IEEE Symposium Series on Computational Intelligence (SSCI)*, 2018, pp. 1234–1241.
- [8] M. Granada-Echeverri, L. Cubides, and O. Bustamante, "The electric vehicle routing problem with backualls," *International Journal of Industrial Engineering Computations*, vol. 10, pp. 1–22, 2019.
- [9] T. Erdelić and T. Carić, "A survey on the electric vehicle routing problem: variants and solution approaches," *Journal of Advanced Transportation*, vol. 2019, 2019.
- [10] M. Mavrouniotis, C. Menelaou, S. Timotheou, C. Panayiotou, G. Ellinas, and M. Polycarpou, "Benchmark set for the IEEE WCCI-2020 competition on evolutionary computation for the electric vehicle routing problem," KIOS CoE, University of Cyprus, Cyprus, Tech. Rep., 2020.
- [11] M. Mavrouniotis, C. Menelaou, S. Timotheou, G. Ellinas, C. Panayiotou, and M. Polycarpou, "A benchmark test suite for the electric capacitated vehicle routing problem," in *2020 IEEE Congress on Evolutionary Computation (CEC)*, 2020, pp. 1–8.
- [12] S. Pelletier, O. Jabali, and G. Laporte, "50th anniversary invited article—goods distribution with electric vehicles: Review and research perspectives," *Transportation Science*, vol. 50, no. 1, pp. 3–22, 2016.
- [13] M. Dorigo and L. M. Gambardella, "Ant colony system: A cooperative learning approach to the traveling salesman problem," *IEEE Transactions on Evolutionary Computation*, vol. 1, no. 1, pp. 53–66, 1997.
- [14] L. M. Gambardella, A. E. Rizzoli, F. Oliverio, N. Casagrande, A. Donati, R. Montemanni, and E. Lucibello, "Ant colony optimization for vehicle routing in advanced logistics systems," in *Proceedings of the International Workshop on Modelling and Applied Simulation*, 2003, pp. 3–9.
- [15] A. E. Rizzoli, R. Montemanni, E. Lucibello, and L. M. Gambardella, "Ant colony optimization for real-world vehicle routing problems," *Swarm Intelligence*, vol. 1, no. 2, pp. 135–151, 2007.
- [16] S. Erdoğan and E. Miller-Hooks, "A green vehicle routing problem," *Transportation Research Part E: Logistics and Transportation Review*, vol. 48, no. 1, pp. 100–114, 2012.
- [17] A. Froger, J. E. Mendoza, O. Jabali, and G. Laporte, "Improved formulations and algorithmic components for the electric vehicle routing problem with nonlinear charging functions," *Computers & Operations Research*, vol. 104, pp. 256–294, 2019.
- [18] H. Wang, S. Yang, W. Ip, and D. Wang, "A memetic particle swarm optimisation algorithm for dynamic multi-modal optimisation problems," *International Journal of Systems Science*, vol. 43, no. 7, pp. 1268–1283, 2012.
- [19] Y. Mei, K. Tang, and X. Yao, "A memetic algorithm for periodic capacitated arc routing problem," *IEEE Transactions on Systems, Man, and Cybernetics, Part B (Cybernetics)*, vol. 41, no. 6, pp. 1654–1667, 2011.
- [20] M. Mavrouniotis, F. M. Müller, and S. Yang, "Ant colony optimization with local search for the dynamic travelling salesman problems," *IEEE Transactions on Cybernetics*, vol. 47, no. 7, pp. 1743–1756, 2017.
- [21] R. Shang, K. Dai, L. Jiao, and R. Stolk, "Improved memetic algorithm based on route distance grouping for multiobjective large scale capacitated arc routing problems," *IEEE Transactions on Cybernetics*, vol. 46, no. 4, pp. 1000–1013, 2016.
- [22] T. Stützle and H. Hoos, " \mathcal{MAA}^X - \mathcal{MLN} ant system and local search for the traveling salesman problem," in *Proceedings of 1997 IEEE International Conference on Evolutionary Computation*, 1997, pp. 309–314.
- [23] M. Mavrouniotis, C. Li, G. Ellinas, and M. Polycarpou, "Parallel ant colony optimization for the electric vehicle routing problem," in *2019 IEEE Symposium Series on Computational Intelligence (SSCI)*, 2019, pp. 1660–1667.
- [24] Y.-H. Jia, Y. Mei, and M. Zhang, "Confidence-based ant colony optimization for capacitated electric vehicle routing problem with comparison of different encoding schemes," *IEEE Transactions on Evolutionary Computation*, pp. 1–1, 2022.
- [25] —, "A bilevel ant colony optimization algorithm for capacitated electric vehicle routing problem," *IEEE Transactions on Cybernetics*, pp. 1–14, 2021.
- [26] T. Stützle and H. Hoos, "Improvements on the ant-system: Introducing the \mathcal{MAA}^X - \mathcal{MLN} ant system," in *Artificial Neural Nets and Genetic Algorithms*. Vienna: Springer Vienna, 1998, pp. 245–249.
- [27] T. Stützle and H. H. Hoos, " \mathcal{MAA}^X - \mathcal{MLN} ant system," *Future Generation Computer Systems*, vol. 16, no. 8, pp. 889–914, 2000.
- [28] L. M. Gambardella and M. Dorigo, "Ant-Q: A reinforcement learning approach to the traveling salesman problem," in *Machine Learning Proceedings 1995*, A. Prieditis and S. Russell, Eds. San Francisco, CA: Morgan Kaufmann, 1995, pp. 252–260.
- [29] I. Osman, "Metastrategy simulated annealing and tabu search algorithms for the vehicle routing problem," *Annals of Operations Research*, vol. 41, pp. 421–451, 1993.
- [30] S. Lin, "Computer solutions of the traveling salesman problem," *Bell System Technical Journal*, vol. 44, no. 10, pp. 2245–2269, 1965.
- [31] J.-Y. Potvin and J.-M. Rousseau, "An exchange heuristic for routeing problems with time windows," *The Journal of the Operational Research Society*, vol. 46, no. 12, pp. 1433–1446, 1995.
- [32] L. Di Gasparo and A. Schaerf, "Multi-neighbourhood local search with application to course timetabling," in *Practice and Theory of Automated Timetabling IV*, E. Burke and P. De Causmaecker, Eds. Berlin, Heidelberg: Springer Berlin Heidelberg, 2003, pp. 262–275.